



Free-standing photonic glasses with controlled disorder fabricated in a centrifugal field

Received 00th January 20xx,

Mengdi Chen^a, Danja Fischli^a, Lukas Schertel^{b,c}, Geoffroy J. Aubry^b, Benedikt Häusele^a, Sebastian Polarz^a, Georg Maret^b, Helmut Cölfen^{a*}

Accepted 00th January 20xx

DOI: 10.1039/x0xx00000x

www.rsc.org/

One efficient method to obtain disordered colloidal packing is to reduce the stability of colloidal particles by adding electrolytes to the colloidal dispersions. The objective of this paper was to study the effect of CaCl₂ on polystyrene colloidal dispersions and therefore quantitatively instead of empirically control the degree of disorder in the glassy colloidal materials. A threshold concentration of CaCl₂ was found. When exceeding this threshold, different nanoparticle oligomers were observed in the dispersions by analytical ultracentrifugation. Furthermore, macroscopic colloidal assembly was triggered in the centrifugal field and monolithic samples were obtained by polymerizing co-assembled hydrophilic monomers to form a network, which trapped the glassy colloidal structures. Photon time of flight measurements showed that the CaCl₂ concentration threshold should not be exceeded otherwise an optical shortcut may take place. Thus, our work provides a feasible route to prepare macroscopic free-standing photonic glasses with controlled disorder for further optical investigation.

Introduction

Colloidal systems or colloidal dispersions are ubiquitous in both natural environment and industrial processes. In the framework of nanofabrication by bottom-up synthetic chemistry, colloidal dispersions with a continuous liquid phase in which a colloidal solid is dispersed are at the center of interest, due to the design possibilities of many functional

constructs tailored towards a specific purpose by utilizing nanoparticle self-assembly.¹ One of the important uses of such colloidal systems is in photonic applications when the colloidal solid has a size in the order of the light wavelength.^{2,3}

When the solid phase is built up of uniform spherical nanoparticles, for example polymeric latex spheres, regular and periodic arrays known as colloidal crystals are formed under proper conditions. Macroporous materials which are exact inverse replicas of colloidal crystals have been intensively investigated over the past two decades and play an important role in photonic crystal design.⁴

While photonic crystals take advantage of the periodicity in the dielectric constant to provide Bragg scattering of ballistic photons and photonic band gaps, random photonic media known as photonic glasses can also strongly affect light transport and exhibit interesting physical phenomena like random lasing⁵ and possibly light localization. However, contrary to intuition, to obtain high degrees of disorder from monodisperse building blocks is not an easy task. Methods like rapid sedimentation or modified vertical deposition have been proven to be unsuccessful.⁵ Therefore, most experimental work on such random media has been based on materials, which are formed by particles with very broad size or shape distribution⁶⁻⁹ and the individual electro-magnetic response of each building block gives rise to an averaged-out optical response.¹⁰ Resonant behavior of the scattering strength in monodisperse random media was reported¹¹ by which a new scattering regime might be reached in higher refractive index materials. Garcia et al.¹² have done pioneering work and developed two promising routes to fabricate random materials from monodisperse colloidal particles, either by selectively etching one of the two kinds of spheres in a binary colloidal crystals, or by introducing electrolyte to the monodisperse latex spheres dispersion to promote colloidal aggregation.

^a Department of Chemistry, University of Konstanz, Universitätsstr. 10, 78457 Konstanz, Germany. Email: helmut.coelfen@uni-konstanz.de

^b Department of Physics, University of Konstanz, Universitätsstr. 10, 78457 Konstanz, Germany

^c Department of Physics, University of Zürich, Winterthurerstr. 190, 8057 Zürich, Switzerland

Electronic Supplementary Information (ESI) available: [Materials and preparation methods, characterizations, Hamaker software for DLVO calculation]. See DOI: 10.1039/x0xx00000x

However, much knowledge about controlled ways to prepare randomly organized materials is still missing. Although the coagulation route is easy to handle and the coagulation of a charged colloidal dispersion has always been a core aspect of colloidal science,¹³ there is a lack of tools to precisely correlate the amount of electrolyte and the corresponding glassy colloidal packing. In addition, in view of optimizing optical properties, a reliable method to trigger the formation of the glassy colloidal packing as well as to preserve the structure at a macroscopic scale is still a significant challenge and in great demand.

Results and discussion

Figure 1 shows the colloidal packing obtained from drying an aqueous monodisperse polystyrene colloidal dispersion under gravity. It can be easily found that the degree of disorder in the colloidal packing increases as the amount of CaCl₂ increases. When there is no salt present in the polystyrene dispersion, an ordered fcc arrangement was observed, as illustrated in Figure 1a. In the presence of electrolyte, the stability of a colloidal dispersion in which the colloidal particles are electrically charged decreases due to the charge screening by the electrolyte. The degree of order is getting lower and thus more voids are introduced when the concentration of CaCl₂ increased from 5.3mM (Figure 1b) to 10.7mM (Figure 1c).

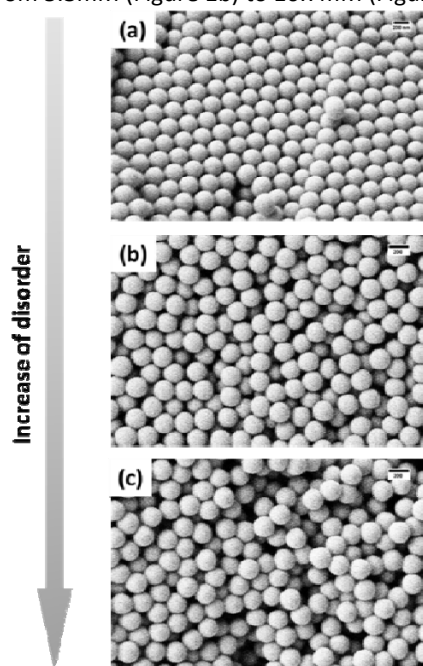


Figure 1. SEM images of colloidal packing obtained by drying a colloidal dispersion with different electrolyte concentration (a) no CaCl₂; (b) 5.3 mM CaCl₂; (c) 10.7mM CaCl₂ under gravity. Scale bar = 200 nm.

Zeta (ξ) potential measurement is a conventional method to characterize the electrostatic stability of colloidal dispersions. When the magnitude of the zeta potential is small, attractive forces may exceed the electric repulsion between adjacent particles and the particles may aggregate and flocculate. Zeta potential measurements of the polystyrene colloidal

dispersions at different concentrations of CaCl₂ are shown in Figure S1a. It can be seen that up to a concentration of CaCl₂ of 10.7 mM, the zeta potential remains smaller than -40 mV which indicates that the colloidal dispersions have a good stability.^{14, 15} However, this does not very well correlate with what is observed in Figure 1 as the colloidal packing already started to lose its order at much lower electrolyte concentration.

Besides the Zeta potential measurements, there are several well-established methods to determine the stability of nanoparticles that can also be assessed via the size of the nanoparticle aggregates and to provide information concerning their surface modification. Dynamic light scattering (DLS) is one of the most widespread methods for sizing nanoparticles. We adopted it here trying to correlate the electrolyte concentration and the colloidal aggregate size. The results from DLS measurements are shown in Figure 2a. There is a small fluctuation in the particle sizes when small amounts of CaCl₂ were present. The average size increases at 10.7 mM indicating aggregation although Fig. 1 shows disorder already at lower electrolyte concentrations. Size distributions from DLS alone are nontrivial to obtain without prior knowledge of whether aggregation is occurring.¹⁶

In contrast, analytical Ultracentrifugation (AUC) is very well suited to detect low levels of aggregation, since it combines an extremely high resolution up to Angstrom resolved particle size distributions¹⁷ with high statistical accuracy because every particle is detected. In figure 2b, the $g^*(s)$ analysis has been used to calculate the sedimentation coefficient distribution.¹⁸ Besides the primary peak, distinct peaks were found while the CaCl₂ concentrations increased. These distinct peaks might intuitively belong to different oligomers of the colloidal particles.

It is relatively straightforward to convert a sedimentation coefficient distribution into a particle size distribution assuming hard spheres using equation (1):

$$d_p = \sqrt{\frac{18\eta_s s}{(\rho_p - \rho_s)}} \quad (1)$$

where d_p is the diameter of the particle, η_s is the viscosity of the medium, s is the sedimentation coefficient, ρ_s is the density of solvent and ρ_p is the density of the particle (1.054 g/ml). By calculating the sedimentation coefficients of the oligomeric structures¹⁹ from the sedimentation coefficient of the monomer (2088 Svedberg), the values shown in table 1 are obtained. In figure 2b, when the CaCl₂ concentration is 9 mM, one species with the sedimentation coefficient of 3030 Svedberg showed up. But this species cannot be assigned to any of the oligomers in Table 1. The species at 3030 Svedberg is more pronounced and a lot more distinct peaks including dimer, trimer triangle, trimer linear, tetramer square, tetramer linear were observed when the concentration of CaCl₂ was increased to 11.3 mM (Figure 3b blue curve). When the concentration of CaCl₂ went even higher to 12.4 mM, the primary peak was weakened while the other oligomer species

cannot be very well distinguished anymore. For easier comparison with other results, the sedimentation coefficients in figure 2b and table 1 were also converted to particle size (Figure 2c) via equation (1). By combining the DLS and AUC analysis, it can be deduced that the polystyrene colloidal system experienced a transformation to a broad aggregate distribution when the concentration of CaCl_2 exceeded a certain threshold around 11 mM.

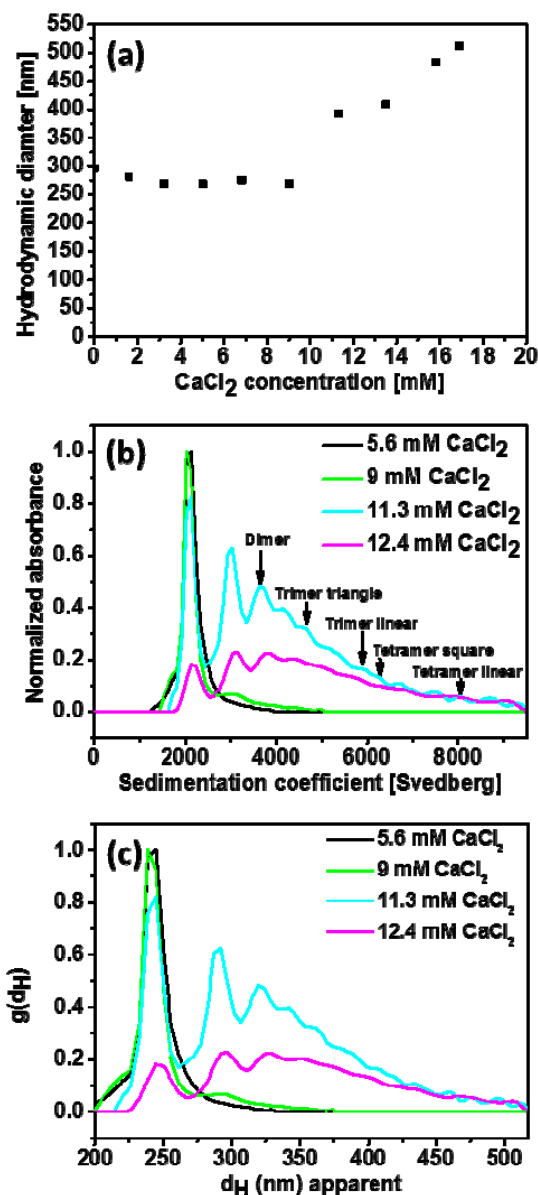


Figure 2. Determination of polystyrene particle sizes to detect the nanoparticle aggregation. (a) The hydrodynamic diameter of the polystyrene colloidal particles measured by dynamic light scattering (DLS) at different electrolyte concentrations; (b) The sedimentation coefficient distribution of the polystyrene colloidal particles measured by analytical ultracentrifugation (AUC) with different electrolyte concentrations; (c) Particle size distribution converted from sedimentation coefficient distribution.

Table 1. Sedimentation coefficient and hydrodynamic diameter of different polystyrene particle oligomers calculated from the sedimentation coefficient of the monomer.¹⁹

	Dimer	Trimer (triangle)	Trimer (linear)	Tetramer (square)	Tetramer (tetrahedron)	Tetramer (linear)
Sedimentation coefficient / [Svedberg]	3712	4793	5800	6207	5611	8028
Hydrodynamic diameter / [nm]	323	367	404	418	397	475

Asymmetrical-Flow-Field-Flow Fractionation (AF4) investigations (Figure S2) of the sample at 11.3 mM Ca^{2+} , which only depend on the particle size, unlike size and density in AUC, did not show any species between monomer (250 nm) and dimer (350 nm). This means that the 3030 S species observed in AUC must be a monomer species with a higher density or a dimer with a lower density. Since the latexes are charge stabilized with sulfonate surface groups, binding of Ca^{2+} will occur, which not only leads to the observed oligomerization but also to a density increase. This is the likely explanation for the 3030 S species. Since it is relatively defined, we suspect that this species results from charge reversal by complete Ca^{2+} binding. Its higher density of 1.081 g/ml calculated from the size of 250 nm and $s = 3030$ S using eq. (1) supports this view as well as the fact that this species only becomes visible at higher Ca^{2+} concentrations starting at 9 mM.

In order to approach a macroscopic material with glassy nanostructure, which could be suitable for further optical investigation (e.g. characterization of its resonant optical behavior¹¹), a centrifugal force⁴ which is easy and efficient to trigger colloidal assembly was applied here. The sediment at the bottom of the centrifuge tube was dried and investigated via SEM. One can easily see from figure 3a that the colloidal packing exhibits a two-layer structure when the amount of CaCl_2 is relatively far below the threshold (about 11 mM obtained from DLS measurement shown in Figure 2a). At the top part there were still some crystalline domains present while a random structure was observed at the bottom. This two-layer structure could be better recognized at lower magnification (see Figure S3). Reflecting the AUC analysis in figure 2b, at the chosen Ca^{2+} concentration of 5.3 mM, the observed structure was built up by monomer nanoparticles, which however already have a tendency to aggregate. This becomes especially evident at the higher particle concentrations near the bottom of the centrifuge tube, where the particles are forced into the primary minimum in the DLVO curve before they are able to form an ordered structure, which they would do in absence of salt. Nevertheless, at the lower particle concentrations at the top of the tube, still ordered domains can be formed (see Figure 3a).

If the amount of CaCl_2 is slightly increased, the dense monomer nanoparticles (3030 S) should be formed. Thus, more glassy domains were observed in figure S4. The SEM

images of colloidal packing prepared at 7.2 mM and 10.1 mM CaCl_2 confirm this transition. It can be found that the glassy domains occupied most of the sample at 7.2 mM CaCl_2 while still some tiny crystalline parts can be found at the top of the sample. But when the concentration of CaCl_2 was increased to 10.1 mM, crystalline domains can be very hardly found (figure S4).

Furthermore, when the amount of CaCl_2 exceeded the threshold, not only the two-layer structure disappeared but the whole structure shown in figure 3b exhibited a random packing with a lot of empty voids. This is caused by the different oligomers formed in presence of high CaCl_2 concentration. Therefore, it can be concluded that a random closed packed colloidal packing could be achieved by adding CaCl_2 to a concentration near but not exceeding the threshold concentration.

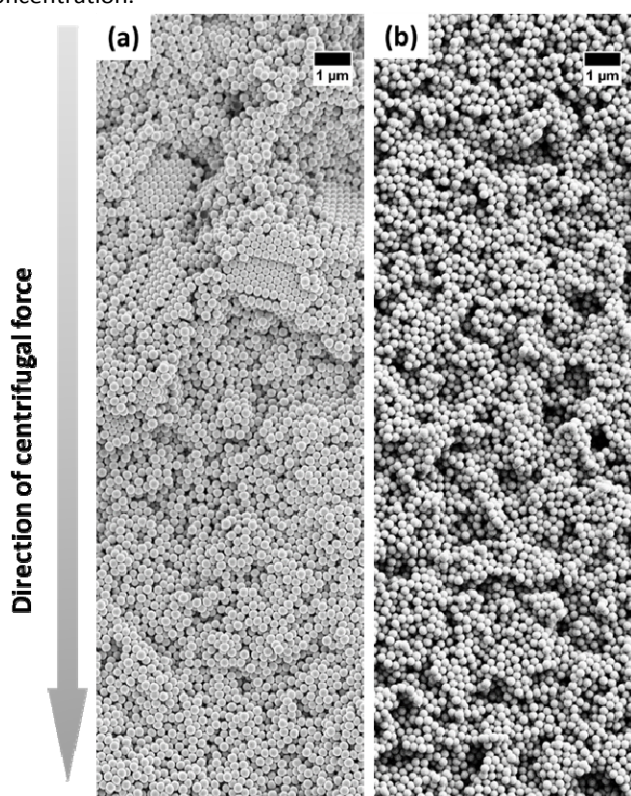


Figure 3. SEM images of colloidal glassy nanostructure prepared in centrifugal field in presence of (a) 5.3mM (b) 13.2 mM CaCl_2 .

Exceeding the threshold leads to holes (see figure 3b) and thus to lower filling fraction. This might affect the light transport (weaker scattering) and lead to almost empty regions (holes) in the macroscopic sample where the light can propagate ballistically. The quality of the macroscopic samples can be characterized in photon time of flight experiments. A very short laser pulse (250 fs) is sent on the sample and a time resolved photodetector measures in transmission for how long the photons traveled through the sample. If no holes are present, the photon transport through the sample follows a diffusion law. The time of flight distribution of a purely diffusive sample is known theoretically and fits the experiments very well⁹. If holes are present in the sample, the

photons entering these holes are much faster (they are not scattered until they exit the hole) and the overall transport through the sample is affected: the time of flight distribution does not follow a diffusion law anymore, some photons leave the sample earlier than expected. This is why holes in such samples are called optical shortcuts. To perform such measurements, as well as to carry out all other optical measurements, free-standing materials with a proper size (1 mm to 1 cm) are needed. However, the colloidal assembly structures are in general quite fragile. Free-standing macroscopic materials are highly in demand to perform the time of flight measurements.

In order to preserve the very fragile colloidal assembly structures, we introduced here a co-assembly method. A hydrophilic monomer, in the present case acrylamide, was added into the colloidal dispersion. The co-assembled structures were polymerized after centrifugation by addition of ammonia persulfate as initiator. So the polystyrene colloidal spheres were trapped in the hydrogel. The robust hydrogel (see Figure S5) can be easily taken out of the centrifuge tube and cut into the desired shape. Images of the monolithic samples can be found in Figure S6a. The samples are on centimeter scale, therefore big enough to perform optical measurements. In figure S6b, c, it can be seen that the amount of polyacrylamide in between the polystyrene spheres differs. High concentration of CaCl_2 caused the formation of different oligomers and created big volume fractions of voids (figure S6c). Therefore, more acrylamide monomers accumulated in between the polystyrene spheres and formed a thicker network after the polymerization.

This influences the light transport behavior of such samples. High amounts of monomers, and thus dense networks “connect” the particles optically and lower the scattering strength. In figure 6, the photon time of flight distribution in a purely diffusive sample (e.g. the one of figure 5a) is shown in black. It can be easily distinguished from the sample of figure 5b, which has optical shortcuts (red curve). They emerge as the early peak seen in the red curve. The blue curve shows the time of flight of photons through a sample with at least one big optical shortcut (for example a crack in the sample): almost all photons went through it and exit the sample very fast.

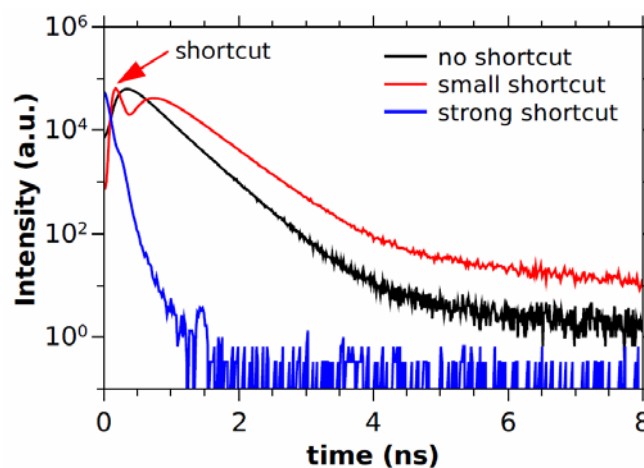


Figure 6. Photon time of flight measurements⁹ distinguishing samples with some big optical shortcuts (blue curve: the photons go out of the sample very early), some smaller optical shortcuts (small early peak in the red curve indicated by a red arrow) and without any optical shortcut (black curve: all the photons behave diffusively)

Conclusions

In this work, we studied the influence of adding CaCl₂ to charge stabilized polystyrene colloidal systems via conventional methods like zeta potential measurement, which could not provide a satisfactory correlation with the observed colloidal packing. Alternatively, we incorporated dynamic light scattering and analytical ultracentrifugation and asymmetrical flow field flow fractionation to characterize the colloidal particle size (distribution) in the presence of different amounts of CaCl₂ and successfully correlated the colloidal systems stability and the formation of different particle oligomers to the corresponding macroscopic colloidal packing structures. From the analytical ultracentrifugation analysis, a defined species, which was heavier than monomer particles appeared and became pronounced when the concentration of CaCl₂ increased to a certain threshold, which can be obtained by dynamic light scattering. When the amount of CaCl₂ was above this threshold, different oligomers of single polystyrene colloidal spheres were formed. To realize a random closed packed colloidal packing, the amount of CaCl₂ should be limited to the threshold to avoid the formation of the oligomers. Therefore, it is possible to predict the kind of packing in the colloidal glass using the sedimentation coefficient distribution from AUC. Furthermore, random colloidal packing was triggered by centrifugal force and very well preserved on a macroscopic scale by trapping the random structure in a hydrogel. Photon time of flight measurements allowed us to characterize the macroscopic optical homogeneity of the samples prepared with different amounts of CaCl₂. Therefore, the fabrication route developed in this work provides a promising materials basis for further optical investigations. This may be relevant for experimental studies of fundamental issues in light transport through random media (see e.g. ^{2,9,11}) but also for novel photonic applications such as diffuse reflectance standards.

Acknowledgements

M.C. is funded by a Chinese Scholarship Council stipend. LS, GJA, GM and HC acknowledge support from the Center for Applied Photonics (Universität Konstanz), GJA acknowledges support from the Zukunftskolleg (Universität Konstanz) for an Independent Research Start-up Grant.

Notes and references

- G. A. Ozin, K. Hou, B. V. Lotsch, L. Cademartiri, D. P. Puzzo, F. Scotognella, A. Ghadimi and J. Thomson, *Materials Today*, 2009, **12**, 12-23.
- D. S. Wiersma, *Nature Photonics*, 2013, **7**, 188-196.
- S.-H. Kim, S. Y. Lee, S.-M. Yang and G.-R. Yi, *NPG Asia Materials*, 2011, **3**, 25-33.
- G. von Freymann, V. Kitaev, B. V. Lotsch and G. A. Ozin, *Chemical Society Reviews*, 2013, **42**, 2528-2554.
- P. D. García, R. Sapienza and C. López, *Advanced materials*, 2010, **22**, 12-19.
- N. M. Lawandy, R. Balachandran, A. Gomes and E. Sauvain, *Nature*, 1994, **368**, 436-438.
- L. F. Rojas-Ochoa, J. Mendez-Alcaraz, J. Sáenz, P. Schurtenberger and F. Scheffold, *Physical review letters*, 2004, **93**, 073903.
- M. Reufer, L. F. Rojas-Ochoa, S. Eiden, J. J. Sáenz and F. Scheffold, *Applied Physics Letters*, 2007, **91**, 171904.
- T. Sperling, L. Schertel, M. Ackermann, G. J. Aubry, C. M. Aegerter and G. Maret, *New Journal of Physics*, 2016, **18**, 013039.
- J. F. Galisteo - López, M. Ibsate, R. Sapienza, L. S. Froufe - Pérez, Á. Blanco and C. López, *Advanced Materials*, 2011, **23**, 30-69.
- P. Garcia, R. Sapienza, J. Bertolotti, M. Martin, A. Blanco, A. Altube, L. Vina, D. Wiersma and C. López, *Physical Review A*, 2008, **78**, 023823.
- P. D. García, R. Sapienza, Á. Blanco and C. López, *Advanced Materials*, 2007, **19**, 2597-2602.
- S. Xu and Z. Sun, *Soft Matter*, 2011, **7**, 11298-11308.
- B. Salopek, D. Krsić and S. Filipović, *Measurement and application of zeta-potential*, Rudarsko-geološko-naftni fakultet, 1992.
- I. Ostolska and M. Wiśniewska, *Colloid and polymer science*, 2014, **292**, 2453-2464.
- J. B. Falabella, T. J. Cho, D. C. Ripple, V. A. Hackley and M. J. Tarlov, *Langmuir*, 2010, **26**, 12740-12747.
- E. Karabudak, E. Brookes, V. Lesnyak, N. Gaponik, A. Eychmüller, J. Walter, D. Segets, W. Peukert, W. Wohlleben and B. Demeler, *Angewandte Chemie International Edition*, 2016, **55**, 11770-11774.
- J. Lebowitz, M. S. Lewis and P. Schuck, *Protein Science*, 2002, **11**, 2067-2079.
- A. J. R. S.E. Harding, *Dynamic Properties of Biomolecular Assemblies*, ROYAL SOCIETY OF CHEMISTRY, 1988, chapter 1, page 14.